J. Earth Syst. Sci. (2020)129 81
https://doi.org/10.1007/s12040-020-1358-4

Geochemical signatures of Late Paleocene sandstones from the Sanu Formation, Jaisalmer basin, western India: Implication for provenance, weathering and tectonic setting

A Patra* and Anil D Shukla

Geosciences Division, Physical Research Laboratory, Ahmedabad, Gujarat 380 009, India.
**Corresponding author. e-mail: amitava.geol@gmail.com*

MS received 19 April 2019; revised 18 September 2019; accepted 27 December 2019

Sandstones of the Sanu Formation from Jaisalmer basin, western India were studied for major, trace and rare earth element (REE) geochemistry to deduce their paleo-weathering, tectonic setting, source rock characteristics and provenance. Geochemical results suggest that these sandstones can be classified into sub-arkose, which is supported by petrographic observations. The chemical index of alteration (CIA) values indicate intense chemical weathering. The major, trace and rare earth elements concentration pattern reveals that the sediments of the Sanu Formation were derived from silicic rock sources. The elemental discrimination diagrams specifically $(Gd/Yb)_N$ against Eu/Eu* suggest the Archean provenance as source possibly Aravallis for the studied samples.

Keywords. Geochemistry; provenance; Paleocene; Sanu Sandstone Formation; Jaisalmer basin.

1. Introduction

Geochemical study of the sedimentary rocks has been strongly used to decipher the provenance as well as the tectonic evolution of the sedimentary basins in the past few decades (Pettijohn *et al.* 1972; Dickinson and Suczek 1979; Dickinson 1982, 1985, 1988; Dickinson *et al.* 1983; Potter 1986). Using major and trace elements data from sedimentary rocks has been correlated to plate tectonic setting (Bhatia 1983; Roser and Korsch 1986, 1988; Naqvi *et al.* 1988; McLennan *et al.* 1990; Banerjee and Bhattacharya 1994) as well as to get insights about the tectonic evolution of the terrain. Similarly, the major element chemistry gives clue to the provenance type as well as weathering conditions (Nesbit and Young 1982) which in turn controlled by the tectonic setting of the basin. Certain trace elements and rare earth elements (REE) are most suitable for the determination of provenance and tectonic setting (Bhatia 1983; Taylor and McLennan 1985; Bhatia and Crook 1986), because of their relatively low mobility during sedimentary processes and their low residence time in seawater. These elements are generally thought to be quantitatively transported into clastic sedimentary rocks after weathering, and thus, they may reflect the signature of parent materials.

The Indian subcontinent existed as an isolated landmass, surrounded by the Tethys Sea in the north and the Indian Ocean on the other three sides (Kale 2014) at the beginning of Paleogene. Late Paleocene (57.9–54.7 Ma) witnessed a major transgression on the Indian subcontinent possibly driven by the tectonics of the Ninety East Ridge as

Published online: 26 February 2020

well as the India–Asia collision looks primarily responsible for the major transgression. The tectonic subsidence created accommodation space in the form of pericratonic basins where sedimentation began in the late Paleocene (Singh *et al.* 2016). The early Paleogene (Paleocene–Eocene) has been considered a globally warm period, superimposed on which were several transient hyperthermal events of extreme warmth. The Paleocene Eocene Thermal Maxima (PETM) boundary interval is the most prominent extreme warming episode of 200 Ka duration (Zachos *et al.* 2001). PETM is characterized by 2–6‰ negative carbon isotope excursions in both terrestrial and marine sediment records, worldwide (Zachos *et al.* 2007). In India, Paleogene successions are exposed at a number of places in Tethys and Lesser Himalaya, hills of Meghalaya, Indo-Myanmar range, Arunachal Pradesh, Andaman, Rajasthan, Gujarat and Pondicherry.

The Paleogene succession of the Jaisalmer basin, Rajasthan has hydrocarbon potential. This succession is dominantly represented by calcareous and argillaceous rocks with a subordinate proportion of arenites in the basal part. The global nature of PETM events triggered our thinking to look for the environmental settings during the early Paleogene in this basin, which may provide the clue to the paleoclimatic history of this region. For this purpose, we made an effort to understand the scenario prior to the global PETM event in the Sanu Formation of Jaisalmer basin, which marks the initiation of the basin sedimentations. Here, we are presenting our studies to evaluate the major, trace and rare earth elements geochemistry of the studied Sanu sandstones in order to decipher their provenance, tectonic setting and weathering conditions prevailing in the source region.

2. Geological framework

The Jaisalmer basin is the eastern extension of the shelf part of the Indus basin and represents a more or less central part of the 'West Rajasthan Shelf' tectonic province that is located to the west of the Aravalli ranges in western India, occupies an area of 42,000 km^2 and much of it is covered by the modern sand-dunes (Singh 2007). The basin is differentiated into four geotectonic blocks from north to south. The Kishangarh sub-basin is a part of north-westerly homoclinally gentle dipping shelf with NE–SW depositional strike. The Jaisalmer–Mari high shows upwarping of the basement affecting overlying sediments. This high is a present day gravity high feature located along the shoulder zone of Kanoi fault and is attributed to upthrusting and wrench faulting (Singh 2007). Further, the Shahgarh sub-basin is the deepest depression and is less distributed having NNW–SSE trending faults, while structurally simpler Miajlar sub-basin is located in southern extremity of the basin (Singh 2007). Aravalli Supergroup forms the basement of the Jaisalmer basin containing Mesozoic and Paleogene sequences. The Aravalli–Delhi mountain belt in Rajasthan, is made up of Proterozoic volcano-sedimentary rocks (Sharma 2009). The Aravalli Supergroup has been divided into three sectors such as Bhilwara sector, consisting of amphibolite facies schists, gneisses and migmatites in the northeast, Udaipur sector, consisting of green schist, conglomerate, quartzite, carbonate and metapelite and the southern sector consisting of metapelite, mafic/ultramafic rocks and minor carbonates that are low-grade in the northern part and high-grade in the southern and eastern part (Mohanty and Naha 1986).

Paleogene rocks of the Jaisalmer area are exposed in a crescent shape between Habur and Bandah villages in the north of the Jaisalmer city (figure 1a). The general strike of the beds is in the NW–SE direction and northerly dipping with dip angles 6°–8°. The Paleogene succession of the basin rests over the Mesozoic (Jurassic–Cretaceous) succession that occurs in the southern part as basal beds. The uppermost Cretaceous limestone (Habur Limestone) is unconformably overlain by a meter thick calcrete that represents an unconformity. A major hiatus ranging from upper Cretaceous to lower Paleocene resulted due to a major uplift of the belt (Rahman 1963) and caused considerable erosion of the Cretaceous sediments. The Cenozoic succession begins with late Paleocene cross-bedded, thin bedded and laminated sandstones of Sanu Formation (figure 1b). The cross bedded sandstone facies changes into a medium grain thin bedded type in the middle and later transgressed into fine grain laminated sandstone. The Sanu Formation is overlain by Khuiala Formation, which is comprised of shale and limestones. The basal part of the Sanu Formation consists of a 6 m thick of grey-to-yellow coarse-grained cross bedded sandstone. The thinly bedded sandstone overlies the cross-bedded sandstone. The thickness of this lithofacies is 6 m. This sandstone is grey in the

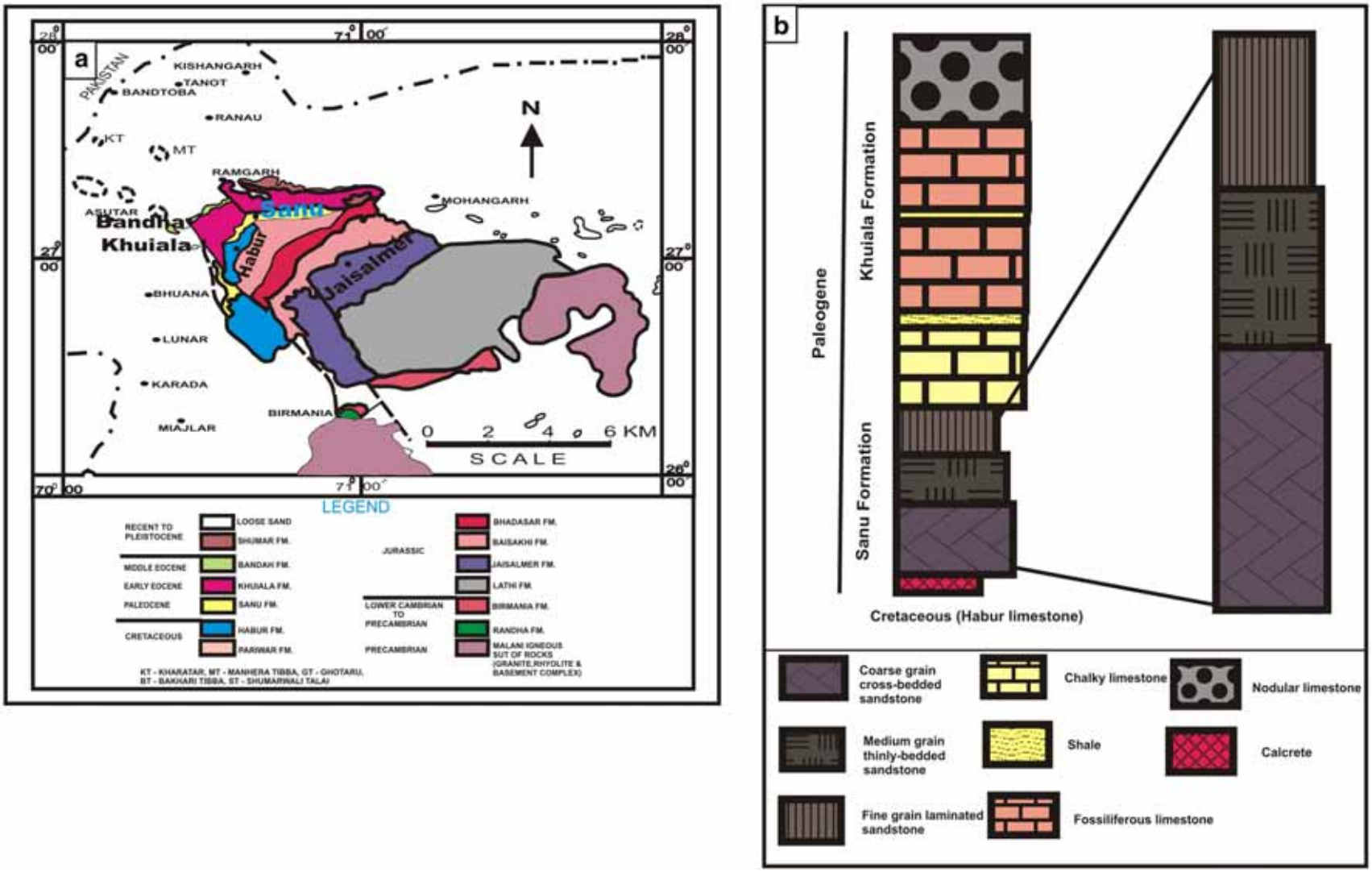

Figure 1. (**a**) Geological map of the Jaisalmer area (after Singh 2007). Note the Paleogene formations in the northern side of the map. (**b**) Litho-column displaying vertical organization of different lithofacies in the Paleogene succession of the Jaisalmer basin, including late Paleocene sandstones.

bottom followed by yellowish brown (ocherous) colour. Individual beds thickness varies from 2 to 4 cm. The laminated sandstone overlies the thinly bedded sandstone. The thickness of this unit is 5 m. Individual lamina thickness varies from 2 to 4 mm. This is fine-grained yellow-to-grey (Patra and Singh 2015).

3. Material and analytical methods

Field study was carried out on the sandstone Members of Sanu Formation in Jaisalmer basin along the Sanu–Ramgarh road section and fresh representative sandstone samples were collected from the study area. The chemical analyses of 10 representative samples were carried out for major, trace and REEs at Physical Research Laboratory, Ahmedabad, India. The major elements analysis was carried out using pressed powder pellet with X-Ray Fluorescence (XRF) technique using Panlytical Axios system. The trace elements and REE were analysed in the sandstone samples along with USGS rock standard BHVO-2 following standard HF–HNO_3 dissolution technique in Savillex Teflon vials. About ∼50 mg powdered samples were dissolved completely using ultra-pure acids. The final solutions were prepared in 2% HNO_3. The analyses were performed on ICAP-Qc on highly diluted samples to avoid matrix effect. The calibration curves were generated using blank and various dilutions of BHVO-2, United States Geological Survey (USGS) standards. The errors in measurements are better than 5% at 2σ level for trace elements analysed. The accuracy check was carried out on different aliquot of BHVO-2 for various dilutions at regular intervals during the analysis (Ray and Shukla 2018).

4. Results and discussion

4.1 *Sandstone petrography*

The petrographic study revealed that the sandstones are characterized by fine to coarse grained detrital quartz with matrix. The framework grains of sandstones are made of quartz, plagioclase, k-feldspar and lithic fragments. Quartz is predominant detrital grain (72–76%, modal composition) and characterised by sub-angular to sub-rounded shape and moderately sorted. The feldspars proportion are (4–5%) with dominance of plagioclase. Rock-fragments are also present which are mainly slate, phyllite and limestone. The sandstones are cemented with both carbonate and ferruginous cement (figure 2). The suite of heavy minerals present in the studied sandstones are magnetite, tourmaline, kyanite, staurolite and zircon (Patra *et al.* 2014).

4.2 *Major oxides*

The major element oxides of the sandstones of Sanu Formation, Jaisalmer basin are presented in table 1. The average SiO_2 content of Sanu sandstones (75.6%) reflects high quartz proportion of these sandstones. Al_2O_3 shows positive correlation with SiO_2, MgO, Na_2O and K_2O and Al_2O_3 shows negative correlation with Fe_2O_3, MnO, CaO, and P_2O_5. Low CaO and Na_2O contents may be contributed by the plagioclases. These studied sandstones contain high SiO_2 and high SiO_2/Al_2O_3 ratio >10, chemical maturity index, average 10.14 (Nesbitt and Young 1982) proposed CIA was based on the calculation in terms of molecular proportion: CIA = $[Al_2O_3/Al_2O_3+CaO^*+Na_2O+K_2O] \times 100$. TiO_2 values in these sandstones suggest derivation from the TiO_2 containing opaque minerals. Moderate proportions of Al_2O_3 indicate presence of clays and micas. Substantial amount of Fe_2O_3 derived from the iron oxide is present as a cementing material in these sandstones. MnO and P_2O_5 proportions in these sandstone samples are low and do not show any significant variation. The major variation occurs in SiO_2, CaO and Fe_2O_3 concentration. The average ratio of Na_2O/K_2O >1 in these sandstone support dominance of plagioclase feldspar. In the geochemical classification diagram of Pettijohn *et al.* (1987), the studied samples occupy the sub-arkose field (figure 3).

4.3 *Trace elements and REEs*

Trace elements and rare earth element (REE) concentrations of sandstone samples from the Sanu Formation are presented in table 2. To understand the trace element concentrations within the sandstone samples, we have compared the data with Upper Continental Crust (UCC). The analysed sandstone samples display relatively similar pattern normalized to UCC with the exception of certain elements (figure 4). The trace elements like Sc, Ni, Cu, Rb, Zn, Sr, Y, Zr and Ba are depleted and Cr and U are enriched in comparison to UCC. The ratios of Rb/Sr and Th/U in analyzed samples

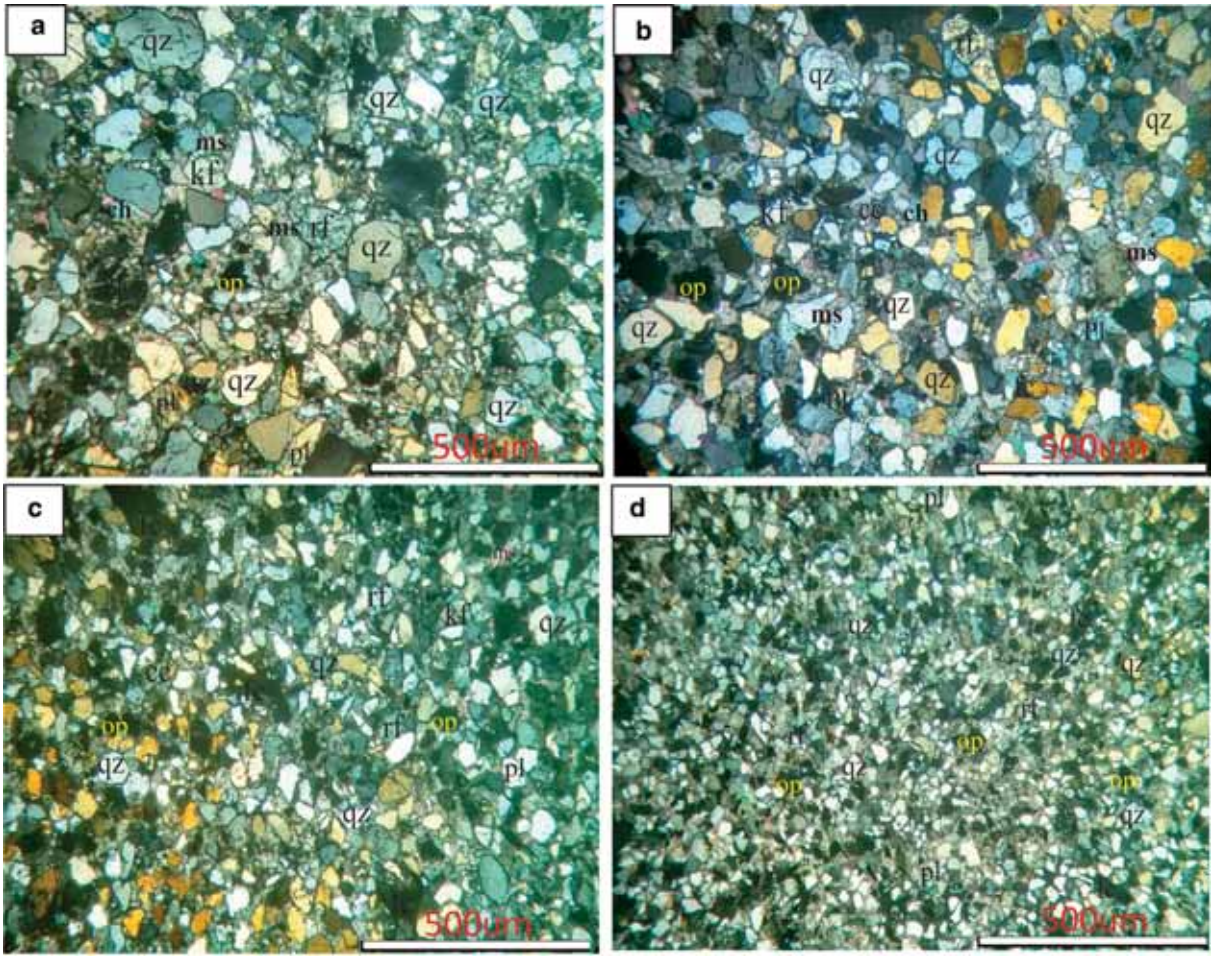

Figure 2. Photomicrographs of sandstone. (**a**) Coarse to medium grained possessing monocrystalline quartz (qz), plagioclase (pl), k-feldspar (kf), rock fragment (rf), opaque (op), chlorite (ch), muscovite (ms) cemented with calcite cement (cc). (**b**) Medium-grained sandstone containing monocrystalline quartz and feldspar cemented by ferruginous cement (fc). (**c**) Medium-grained sandstone containing quartz, feldspar and rock fragments. (**d**) Fine-grained sandstone dominantly containing monocrystalline quartz and subordinate feldspar and rock fragments after Patra *et al.* (2014).

are ranging from 0.01–0.09 and 0.21–4.05, respectively (table 2). The large-ion lithophile elements (LILE), i.e., Rb, Sr, Ba, and Th are showing negative correlation (R^2 = −0.51, −0.23, −0.27, −0.20, respectively) with Al_2O_3. The concentrations of Zr, Hf, and Y (high field strength elements, HFSE) are slightly depleted to those of UCC. Overall ratio of Zr/Hf ranges from 21.8 to 28.5 (table 2) which suggests the presence of heavy minerals in the studied samples (Periasamy and Venkateshwarlu 2017). The correlation coefficient of Zr with Hf is 0.70. The distribution of trace elements in Sanu sandstones show depletion as compared to UCC except Cr and U (figure 4). The depletion of trace element contents in sandstones is apparently induced by the presence of increased amount of quartz that causes overall dilutions (Shukla *et al.* 2019). But Cr, U shows slight enrichment (figure 4), which indicate that these elements may be linked with clay minerals. In sedimentary rocks, Cr may be present in primary detrital phases such as chromite, magnetite and ilmenite. During weathering, the behaviour of Cr^{3+} resembles that of Fe^{3+} and Al^{3+}, leading to widespread accumulation in secondary oxides and clays (Mielke 1979). The positive correlation between U and K_2O ($R^2 = 0.3$) indicate that the concentration of U might be controlled by clay mineral.

We have also reproduced the chondrite normalized REE diagram for clues regarding the sources (figure 5). The data show enrichment of light rare earth element (LREE) compared to heavy rare earth elements (HREE) (figure 5). The total LREE value ranges from 15.5 to 25.5 ppm and total HREE from 0.8 to 1.2 ppm. The average ratio of ΣLREE/ΣHREE in the studied samples is 20.9. The REE pattern shows negative Eu anomaly (Eu/Eu*= 0.7–0.85). There is no significant variation in

Table 1. *Major elements (wt.%) concentration of sandstones in Jaisalmer basin.*

Elements	SA-1	SA-2	SA-3	SA-4	SA-5	SA-6	SA-7	SA-8	SA-9	SA-10	Average values
SiO_2	84.3	83.2	81.8	76.5	75.7	74.8	75.5	73.7	74.2	76.2	77.6
Al_2O_3	7.45	7.44	7.62	7.6	7.38	7.42	7.38	7.39	7.44	7.43	7.45
TiO_2	2.35	2.32	2.12	2.13	2.26	2.17	2.25	2.25	2.21	2.13	2.22
Fe_2O_3	1.79	1.77	1.57	2.29	2.28	2.35	2.89	3.97	4.24	3.57	4.67
MnO	0.01	0.01	0.02	0.02	0.03	0.04	0.03	0.03	0.04	0.04	0.03
CaO	0.98	0.96	0.92	5.77	5.73	5.75	3.83	3.89	3.37	3.82	3.50
MgO	0.19	0.18	0.36	0.33	0.32	0.29	0.24	0.23	0.24	0.23	0.26
Na_2O	0.41	0.38	0.52	0.33	0.42	0.35	0.43	0.35	0.38	0.33	0.39
K_2O	0.32	0.35	0.42	0.41	0.37	0.39	0.35	0.33	0.35	0.43	0.37
P_2O_5	0.06	0.05	0.03	0.03	0.04	0.05	0.03	0.03	0.05	0.04	0.04
L.O.I.	2.02	3.01	4.02	5.75	5.25	5.02	7.32	6.75	8.06	6.25	3.45
Total	99.9	99.7	99.4	101	99.8	98.7	100	99.9	100	100	100
CIA	81.5	82.0	77.9	83.2	80.5	82.5	80.4	83.0	82.0	82.7	82.0
CIW	84.7	85.6	81.7	87.5	84.2	86.6	83.9	86.5	85.6	87.2	85.4
ICV	0.64	0.63	0.65	1.25	1.30	1.28	1.11	1.18	1.14	1.13	1.03
SiO_2/Al_2O_3	11.3	11.2	10.7	9.67	10.3	9.82	9.69	9.57	9.44	9.72	10.1
K_2O/Na_2O	0.78	0.92	0.81	1.24	0.88	1.11	0.81	0.94	0.92	1.30	0.97
Na_2O/K_2O	1.28	1.09	1.24	0.80	1.14	0.90	1.23	1.06	1.09	0.77	1.06

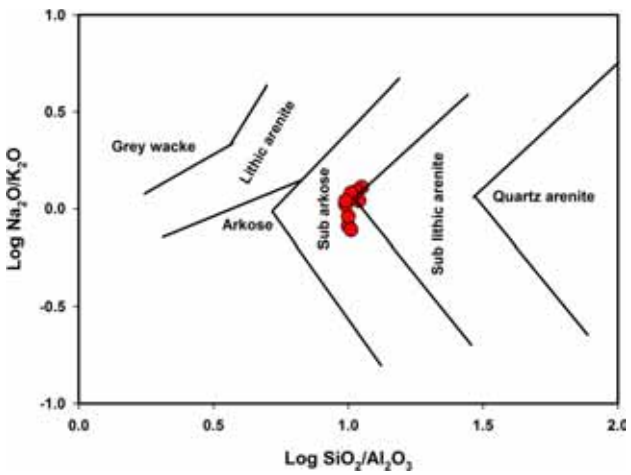

Figure 3. $Log(Na_2O/K_2O)$ *vs.* $Log(SiO_2/Al_2O_3)$ (Pettijohn *et al.* 1987) shows geochemical classification of the Sanu sandstones.

the concentration of ΣREE among the Sanu sandstones. The ratios of Gd_N/Yb_N of the studied sandstones are >2 (2.35–3.12).

4.4 *Palaeoweathering conditions*

The most widely used chemical index to determine the degree of source area weathering is the Chemical Index of Alteration (CIA). Nesbitt and Young (1982) proposed that CIA was based on the calculation in terms of molecular proportion, $CIA=[Al_2O_3/Al_2O_3+CaO^*+Na_2O+K_2O] \times 100$. The CIA values of the sandstones of Sanu Formation range from 77.9% to 83.2% with an average of 82.0%. These values indicate that the sediments were derived from the source rocks that have been subjected to intense chemical breakdown. Many authors have used chemical index of weathering (CIW) for a better estimation of weathering conditions in source area (Fedo *et al.* 1995). The CIW values of the Sanu sandstone ranged from 81.7% to 87.5% with an average of 85.4%. The studied sediments may be subjected to moderate to high chemical weathering on the basis of the CIW.

The A–CN–K (Al_2O_3–CaO^*+Na_2O–K_2O) ternary compositional space diagram shows that the studied sandstones cluster along the A–CN edge. In the initial stage, the weathering trends are parallel to the A–CN line, due to removal of Na and Ca with destruction of plagioclase feldspars. This is shown in figure 6 with a solid arrow starting from the tonalite composition. The continuation of weathering destroyed K-feldspars are releasing K and shifting the residual composition towards Al_2O_3. Additionally, the A–CN–K compositional space estimate that the source rock composition is possible by backward projection of the weathered samples to a point on the feldspar join (McLennan *et al.* 1993). Extrapolation of the weathering trend line intersects the feldspar join and indicates an average source rock composition for the Jaisalmer sandstones between tonalite and granodiorite (figure 6). Hence, the pre-existing lithologies (tonolite/granodiorite) in the Aravalli rocks could

Table 2. *Trace and rare earth elements (ppm) concentration of sandstones in Jaisalmer basin.*

Elements	SA-1	SA-2	SA-3	SA-4	SA-5	SA-6	SA-7	SA-8	SA-9	SA-10	Average values
Sc	4.91	5.02	4.95	5.04	5.12	4.67	4.83	4.75	5.03	5.08	4.94
Cr	109	137	115	51	148	111	114	118	123	125	115.1
Co	5.77	6.06	11.7	7.10	10.1	11.3	11.4	12.0	11.6	10.7	9.77
Ni	8.13	10.4	24.0	11.3	18.6	22.8	22.5	17.8	12.5	18.3	16.6
Cu	4.99	5.69	7.53	4.87	5.88	7.00	7.10	5.62	4.85	6.75	6.03
Zn	11.3	33.4	15.4	10.8	24.4	15.0	23.4	12.2	21.3	17.8	18.5
Rb	1.49	1.64	1.10	0.83	2.31	1.01	1.04	1.72	2.24	2.12	1.55
Sr	16.3	20.9	68.0	30.0	69.2	64.3	65.5	62.3	65.4	66.3	52.8
Y	2.52	2.74	2.76	2.71	3.16	2.65	2.66	3.12	2.53	2.82	2.77
Zr	14.1	17.4	18.2	20.0	21.1	18.0	17.5	15.9	16.6	17.5	17.6
Nb	1.82	1.93	2.27	1.76	3.55	2.11	2.29	2.72	1.85	2.12	2.24
Cs	2.58	4.19	5.17	5.42	4.80	4.70	4.84	4.52	5.15	2.55	4.39
Ba	20.7	23.2	46.1	17.5	36.2	43.1	44.5	42.1	35.7	41.7	35.1
Hf	0.61	0.70	0.70	0.74	0.74	0.68	0.67	0.62	0.76	0.65	0.69
Ta	0.11	0.12	0.14	0.11	0.20	0.13	0.14	0.15	0.11	0.21	0.14
Pb	3.04	4.89	4.73	4.33	3.78	3.90	4.41	4.35	3.92	4.75	4.21
Th	0.85	1.13	1.60	1.18	2.28	1.35	1.26	1.52	1.43	1.54	1.41
U	0.21	0.29	5.90	1.62	2.76	5.60	5.95	3.35	2.15	1.65	2.95
Rb/Sr	0.09	0.08	0.02	0.03	0.03	0.01	0.01	0.03	0.03	0.03	0.04
Zr/Hf	23.1	24.9	26.0	27.1	28.5	26.5	26.2	25.6	21.8	27.0	25.5
Th/U	4.05	3.90	0.27	0.73	0.83	0.24	0.21	0.45	0.66	0.93	1.23
La	2.66	3.30	4.57	3.12	4.25	3.96	3.88	3.35	3.75	4.15	3.69
Ce	7.58	8.87	11.6	9.16	11.5	10.5	10.0	9.25	8.85	12.1	10.0
Pr	0.70	0.86	1.33	1.01	1.12	1.20	1.16	0.89	1.15	0.75	1.02
Nd	3.01	3.57	5.66	4.31	4.65	5.25	5.09	5.17	4.52	4.72	4.59
Sm	0.65	0.76	1.12	0.93	0.91	1.04	1.03	0.92	1.05	0.95	0.94
Eu	0.20	0.22	0.26	0.24	0.25	0.25	0.24	0.23	0.26	0.27	0.24
Gd	0.67	0.77	0.93	0.85	0.92	0.88	0.90	0.95	0.78	0.86	0.85
Dy	0.35	0.41	0.45	0.48	0.51	0.42	0.42	0.43	0.52	0.53	0.45
Er	0.22	0.25	0.26	0.26	0.29	0.24	0.24	0.23	0.25	0.28	0.25
Tm	0.03	0.04	0.04	0.04	0.04	0.03	0.03	0.05	0.04	0.03	0.04
Yb	0.23	0.24	0.25	0.24	0.28	0.24	0.23	0.28	0.25	0.23	0.25
Lu	0.04	0.04	0.04	0.04	0.04	0.04	0.04	0.05	0.03	0.04	0.04
ΣREE	16.3	19.3	26.5	20.7	24.8	24.1	23.3	21.9	21.4	24.9	22.3
ΣLREE	15.5	18.3	25.5	19.6	23.6	23.1	22.3	20.8	20.4	23.8	21.3
ΣHREE	0.8	1.0	1.0	1.1	1.2	1.0	1.0	1.1	1.0	1.1	1.03
LREE/HREE	19.4	18.3	25.5	17.8	19.7	23.1	22.3	20.8	20.4	21.6	20.9
Gd_N/Yb_N	2.35	2.56	2.94	2.85	2.64	2.89	3.12	2.71	2.50	2.99	2.76

have been controlling the composition of the Sanu Sandstones.

4.5 *Sediment sorting and recycling*

Clastic sediments undergo hydraulic/mechanical sorting during transportation which significantly influences the bulk chemical composition of the resultant rocks by enriching certain minerals due to fractionation (Cullers *et al.* 1979; McLennan 1989; Bauluz *et al.* 2000; Armstrong-Altrin 2009; Singh 2009; Wu *et al.* 2013). Index of compositional variability [$(Fe_2O_3+K_2O+Na_2O+CaO+MgO+MnO+TiO_2)/Al_2O_3$, ICV] is used to study the geochemical variability due to hydraulic sorting (Cox *et al.* 1995). Generally, ICV values >0.84 show the presence of rock forming minerals, while <0.84 is characteristic of altered products, *viz.*, clay minerals (Cox *et al.* 1995; Cullers 2000; Armstrong-Altrin *et al.* 2014). The ICV value of the studied samples are >0.84 (average 1.0334, table 1), which suggests the enrichment of primary minerals. In addition, ICV > 1 is suggestive of first cycle of sediments, which is well reflected in

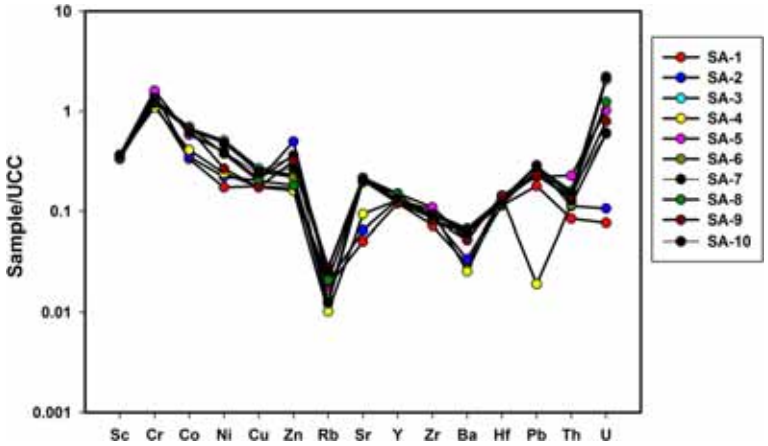

Figure 4. Plot of upper continental crust normalized trace element patterns of Sanu sandstones.

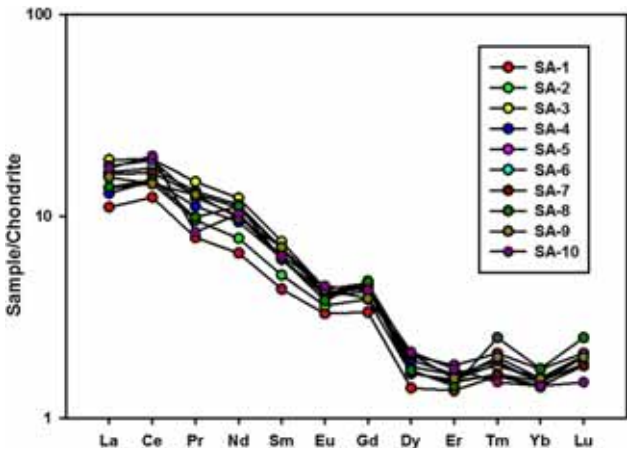

Figure 5. Chondrite normalized REE patterns of Sanu sandstones.

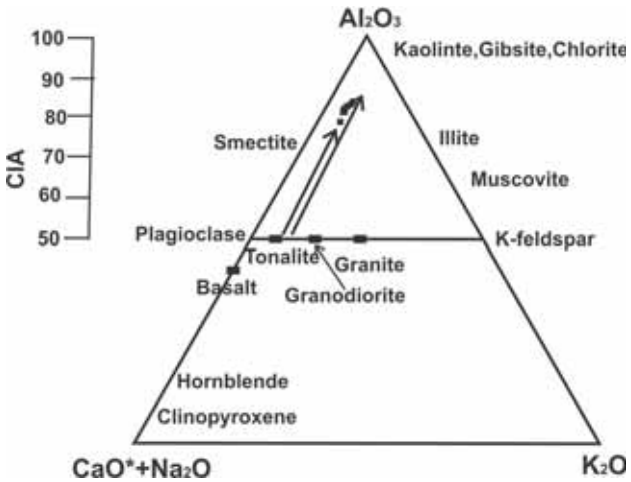

Figure 6. A–CN–K (in molecular proportion) ternary plot (Nesbitt and Young 1982) for the Sanu sandstones.

studied samples under the microscopes. Also, SiO_2/Al_2O_3 ratio is calculated to know the textural maturity of sediments, higher SiO_2/Al_2O_3 (average 10.1) values indicate maturity of sediments (Ahmad and Chandra 2013; Armstrong-Altrin *et al.* 2014). The SiO_2/Al_2O_3 ratio of the studied samples varies from 9.44 to 11.3; infer that these sediments are matured.

The concentration of high weathering resistant phases (like zircon) in the samples can reflect the sorting and recycling processes involved (Armstrong-Altrin *et al.* 2012). In general, Zr/Sc ratio increases by addition of zircon mineral during sorting and/or recycling processes (McLennan *et al.* 1993; Armstrong-Altrin *et al.* 2012). The positive correlation of Zr against Th ($R^2 = 0.65$) and Zr against total REE ($R^2 = 0.58$), indicate significant influence of sorting and recycling of sediments. Hence, it can be interpreted that both grain-size fraction and heavy mineral (zircon) content are responsible for difference in contents of total REE in the Sanu sandstone samples.

4.6 *Tectonic setting*

On the Q–F–L and Qm–F–Lt diagram of Dickinson and Suczek (1979), the samples of the Sanu Formation fall within the craton interior and transitional continental field as shown in figure 7, suggest that stable craton supplied sediments to the depositional basin and lithic fragments were contributed locally (Patra *et al.* 2014).

The major and trace elements discrimination diagram has been used extensively to understand the tectonic setting of the sedimentary basins. Bhatia (1983) and Bhatia and Crook (1986) categorized sedimentary basins into four namely oceanic island arc, continental island arc, active continental margin and passive continental margin. In the K_2O/Na_2O *vs.* SiO_2 diagram (figure 8a) (Roser and Korsch 1986), all the studied samples

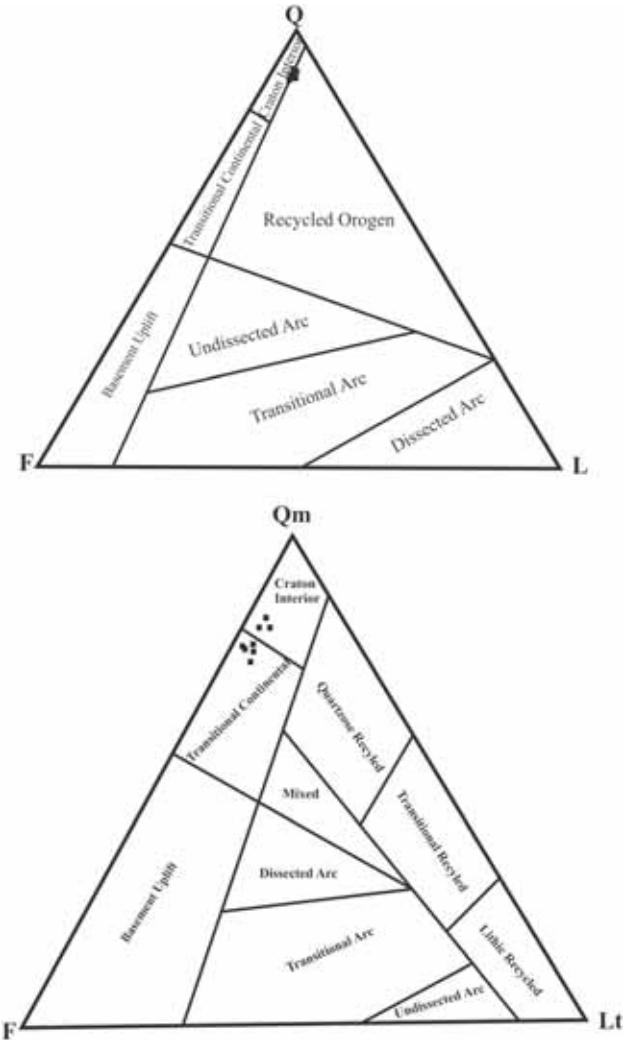

Figure 7. Q–F–L and Qm–F–Lt diagram (after Dickinson *et al.* 1983) of the late Paleocene sandstones of the Jaisalmer basin (Patra *et al.* 2014).

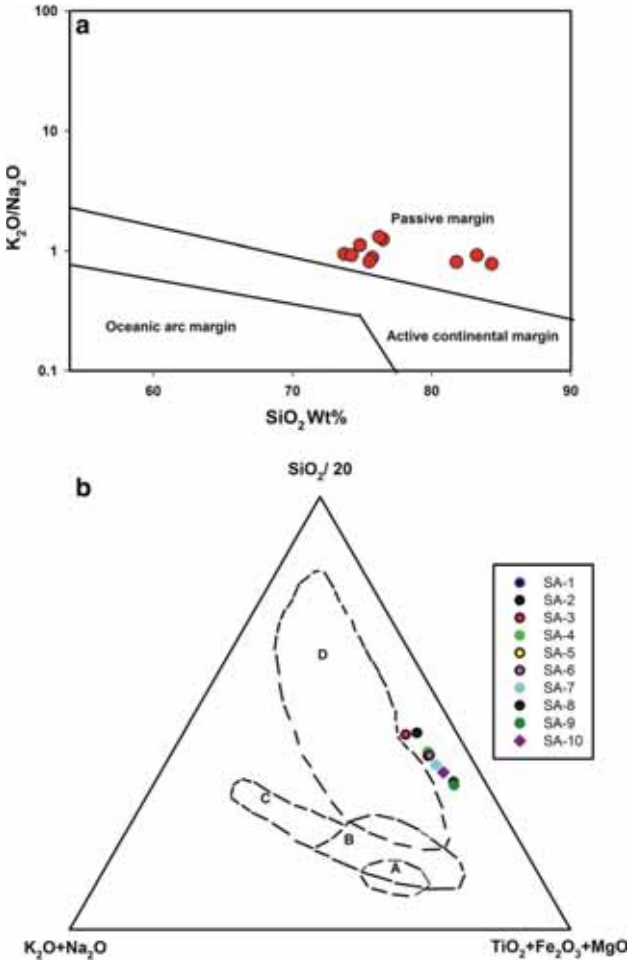

Figure 8. (**a**) Tectonic setting discrimination diagram for Sanu sandstone after Roser and Korch (1986). (**b**) Tectonic discrimination diagram based on major elements composition of the Sanu sandstones after Kroonenberg (1994). A: Ocean Island Arc, B: Continental Island arc, C: Active continental margin, D: Passive margin.

occupy fields of passive margin. This is also supported by (SiO_2/20, K_2O + Na_2O) and (TiO_2 + Fe_2O_3 + MgO) plot of Kroonenberg (1994), (figure 8b).

Certain immobile trace elements (for example, La, Th, Y, Sc, Cr and Zr) have been used extensively to discriminate tectonic settings of clastic sediments (Bhatia and Crook 1986; Sun *et al.* 2012; Yang *et al.* 2012; Jorge *et al.* 2013), a few has been reproduced here to identify the tectonic settings. The bivariate plot of Sc/Cr *vs.* La/Y (figure 9) indicates that Sanu sandstone samples were deposited in a passive continental margin settings since most of the samples fall within the passive field, which is consistent with the plots based on the framework grains (figure 7) major elements (figure 8).

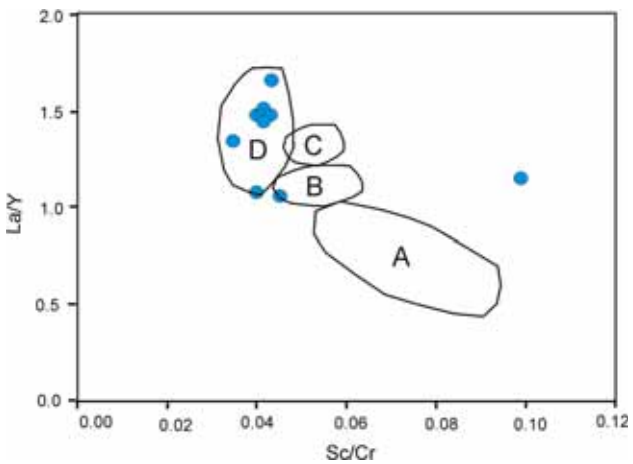

Figure 9. Sc/Cr *vs.* La/Y plot of the Sanu sandstones (after Bhatia and Crook 1986). A: Oceanic Island Arc, B: Continental Island Arc, C: Active Continental Margin, and D: Passive Continental margin settings.

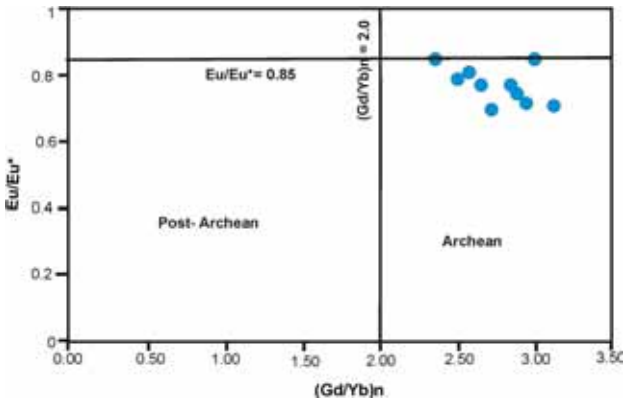

Figure 10. Plot of $(Gd/Yb)_N$ against Eu/Eu* of the Sanu samples (after McLennan and Taylor 1991).

4.7 *Provenance*

The petrography along with paleocurrent analysis in the Sanu sandstones by Patra *et al.* (2014) suggest that the main provenance was in the SE direction of the depositional basin, i.e., Aravalli belt.

The REEs are most widely used as an indicator of the source rock composition because they are virtually insoluble and immobile during sedimentary processes and preserve the signature of the source rock (Taylor and McLennan 1985; Cullers 1995; Armstrong-Altrin *et al.* 2014, 2015). Generally, low LREE/HREE ratios and small/absence of Eu anomalies are indicative of basic rock source, whereas higher ratio and negative Eu anomaly indicate the silicic igneous rock sources (Cullers *et al.* 1987; Cullers 1994). The samples of the Sanu sandstones show high ratio of LREE/HREE (average 19.4) and negative Eu anomaly (figure 5) indicate silicic source rock. The ratio of Gd_N/Yb_N indicates the nature of source rocks composition of the continental crust (Taylor and McLennan 1985). The plot Eu/Eu∗ *vs.* $(Gd/Yb)_N$ (after McLennan and Taylor 1991) in figure 10 with the ratio of $Gd_N/Yb_N = >2$, shows that all the samples fall within Archean field, which suggest that the Archean rocks could act as source rock.

So, the geochemistry suggests that most of the late Paleocene sediments of Jaisalmer basin are materials derived from silicic rocks of the Aravalli Super group.

5. Conclusions

(1) A comprehensive analysis based on geochemistry (major, trace and REE elements) were performed on the sandstones of the Sanu Formation from Jaisalmer basin to deduce their paleoweathering conditions, tectonic setting, source rock and provenance. The studied sandstone members of the Sanu Formation have been analysed based on geochemical signatures to be sub-arkose type.

(2) The value of CIA (77.9–83.2%) and A–CN–K for all the sandstones suggests high degree of weathering at the source area.

(3) Various tectonic discriminant diagrams based on major and trace elements infer that the studied sandstones were deposited in a passive continental setting.

(4) Geochemical characteristics suggest that the sediments of the Sanu Formation were primarily derived from silicic rocks of the Aravalli Super group.

Acknowledgement

AP acknowledges the technical help of Mr T Nirmal Kumar, during the experimental work.

References

Ahmad I and Chandra R 2013 Geochemistry of loess–paleosol sediments of Kashmir Valley, India: Provenance and weathering; *J. Asian Earth Sci.* **66** 73–89.

Armstrong-Altrin J S 2009 Provenance of sands from Cazones Acapulco, and Bahía Kino beaches, Mexico; *Revista Mexicana de Ciencias Geológicas* **26(3)** 764–782.

Armstrong-Altrin J S, Lee Y I, Kasper-Zubillaga J J, Carranza-Edwards A, Garcia D, Eby G N, Balaram V and Cruz-Ortiz N L 2012 Geochemistry of beach sands along the western Gulf of Mexico, Mexico: Implication for provenance; *Chemie der Erde Geochem.* **72** 345–362.

Armstrong-Altrin J S, Nagarajan R, Lee Y I, Kasper-Zubillaga J J and Cordoba-Saldana L P 2014 Geochemistry of sands along the San Nicolás and San Carlos beaches, Gulf of California, Mexico: Implication for provenance; *Turkish J. Earth Sci.* **23** 533–558.

Armstrong-Altrin J S, Luisa Machain-Castillo Maria, Leticiarosales-Hoz, Arturocarranza-Edwards, Sanchez-Cabeza Joan-Albert and Anacarolinaruiz-Fernández 2015 Provenance and depositional history of continental slope sediments in the southwestern Gulf of Mexico unravelled by geochemical analysis; *Cont. Shelf Res.* **95** 15–26.

Banerjee D M and Bhattacharya P 1994 Petrology and geochemistry of greywackes from the Aravalli Supergroup, Rajasthan, India and the tectonic evolution of a Proterozoic sedimentary basin; *Precamb. Res.* **67** 11–35.

Bauluz B, Mayayo M J, Fernandez-Nieto C and Gonzalez-Lopez J M 2000 Geochemistry of Precambrian and Paleozoic siliciclastic rocks from the Iberian Range (NE Spain):

Implications for source area weathering, sorting, provenance, and tectonic setting; *Chem. Geol.* **168** 135–150.

Bhatia M R 1983 Plate tectonics and geochemical composition of sandstones; *J. Geol.* **91** 611–627.

Bhatia M R and Crook K A W 1986 Trace element characteristics of greywacke and tectonic discrimination of sedimentary basins; *Contrib. Mineral. Petrol.* **92** 181–193.

Cox R, Lowe D R and Cullers R L 1995 The influence of sediment recycling and basement composition on evolution of mudrock chemistry in the south-western United States; *Geochim. Cosmochim. Acta* **59** 2919–2940.

Cullers R L 1994 The controls on the major and trace element variation of shales, siltstones and sandstones of Pennsylvanian–Permian age from uplifted continental blocks in Colorado to platform sediment in Kansas, USA; *Geochim. Cosmochim. Acta* **58(22)** 4955–4972.

Cullers R L 1995 The controls on the major and trace element evolution of shales, siltstones and sandstones of Ordovician to Tertiary age in the Wet Mountain region, Colorado, USA; *Chem. Geol.* **123(1–4)** 107–131.

Cullers R L 2000 The geochemistry of shales, siltstone and sandstones of Pennsylvanian–Permian age, Colorado, USA; Implications for provenance and metamorphic studies; *Lithos* **51** 181–203.

Cullers R L, Chaudhuri S, Kilbane N and Koch R 1979 Rare earths in size fractions and sedimentary rocks of Pennsylvanian–Permian age from the mid-continent of the USA; *Geochim. Cosmochim. Acta* **43** 1285–1302.

Cullers R L, Barrett T, Carlson R and Robinson B 1987 Rare-earth element and mineralogic changes in Holocene soil and stream sediment: A case study in the Wet Mountains, Colorado, USA; *Chem. Geol.* **63** 275–297.

Dickinson W R 1982 Compositions of sandstones in Circum-Pacific subduction complexes and fore-arc basins; *Am. Assoc. Petrol. Geol. Bull.* **66** 121–137.

Dickinson W R 1985 Interpreting provenance relations from detrital modes of sandstones; In: *Provenance of sandstones* (ed.) Zuffa G G, D. Reidel., Dordrecht, pp. 333–361.

Dickinson W R 1988 Provenance and sediment dispersal in relation to paleotectonics and paleogeography of sedimentary basins; In: *New Perspectives in Basin Analysis* (eds) Kleinspehn K L and Paola C, Berlin: Springer-Verlag, pp. 3–25.

Dickinson W R and Suczek C A 1979 Plate tectonics and sandstone compositions; *AAPG Bull.* **63** 2164–2182.

Dickinson W R, Beard L S, Braken Ridge G R, Erjavec J L, Ferguson R C, Inman K F, Knepp R A, Lindberg F A and Ryberg P T 1983 Provenance of North American Phanerozoic sandstones in relation to tectonic setting; *Geol. Soc. Am. Bull.* **94** 222–235.

Fedo C M, Nesbitt H W and Young G M 1995 Unravelling the effects of potassium metasomatism in sedimentary rocks and paleosols, with implications for weathering conditions and provenance; *Geology* **23** 921–924.

Jorge R C G S, Fernandes P, Rodrigues B, Pereira Z and Oliveira J T 2013 Geochemistry and provenance of the Carboniferous Baixo Alentejo Flysch Group, South Portuguese Zone; *Sedim. Geol.* **284–285** 133–148.

Kale V S 2014 *Landscapes and Landforms of India, World Geomorphological Landscapes*; Springer Science Business Media Dordrecht, https://doi.org/10.1007/978-94-017-8029-2_3.

Kroonenberg S B 1994 Effects of provenance, sorting and weathering on the geochemistry of fluvial sands from different tectonic and climatic environments; *Proceedings of 29th International Geological Congress*, Part A, pp. 69–81.

McLennan S M 1989 Rare earth elements in sedimentary rocks: Influence of provenance and sedimentary processes; *Rev. Mineral.* **21** 169–200.

McLennan S M and Taylor S R 1991 Sedimentary rocks and crustal evolution: Tectonic setting and secular trends; *J. Geol.* **99** 1–21.

McLennan S M, Hemming S, McDaniel D K and Hanson G N 1993 Geochemical approaches to sedimentation, provenance, and tectonics; In: *Processes controlling the composition of clastic sediments* (eds) Johnson M J and Basu A, *Geol. Soc. Am. Spec. Paper* **284** 21–40.

Mielke J E 1979 Composition of the Earth's Crust and Distribution of the Elements; In: *Review of Research on Modern Problems in Geochemistry* (ed.) Siegel F R, Paris, International Association for Geochemistry and Cosmo chemistry, *Earth Science Series* **16** 13–37.

Mohanty and Naha 1986 Stratigraphic relations of the Precambrian Rocks in the Salumbar area, south eastern Rajasthan; *J. Geol. Soc. India* **27** 479–493.

Naqvi S M, Sarkar R H, Subba Rao D V, Govil P K and Rao T G 1988 Geology, geochemistry and tectonic setting of Archean greywacke from Karnataka nucleus, India; *Precamb. Res.* **39** 193–216.

Nesbitt H W and Young G M 1982 Early Proterozoic climates and plate motions inferred from major element chemistry of lutites; *Nature* **299** 715–717.

Patra A and Singh B P 2015 Facies characteristics and depositional environment of the Paleocene–Eocene strata of the Jaisalmer Basin, western India; *Carbonate Evaporite* **30** 331–346.

Patra A, Singh B P and Srivastava V K 2014 Provenance of the late Paleocene Sandstones of the Jaisalmer Basin, western India; *J. Geol. Soc. India* **83** 657–664.

Periasamy V and Venkateshwarlu M 2017 Petrography and geochemistry of Jurassic sandstones from the Jhuran Formation of Jara dome, Kachchh basin, India: Implications for provenance and tectonic setting; *J. Earth Syst. Sci.* **126** 44.

Pettijohn F J, Potter P E and Siever R 1972 *Sand and Sandstones*; Springer-Verlag, New York, 241p.

Pettijohn F J, Potter P E and Siever R 1987 *Sand and sandstone*; Springer, New York.

Potter P E 1986 South America and a few grains of sand, Pt. I. Beach sands; *J. Geol.* **94(3)** 301–319.

Rahman H 1963 Geology of Petroleum in Pakistan; Proceedings of 6th W.P.C., Section I, pp. 659–683.

Ray D and Shukla A D 2018 The Mukundpura meteorite, a new fall of CM Chondrite; *Planet. Space Sci.*, https://doi.org/10.1016/j.pss.2017.11.005.

Roser B P and Korsch R J 1986 Determination of tectonic setting of sandstone–mudstone suites using SiO_2 content and K_2O/Na_2O ratio; *J. Geol.* **94** 635–650.

Roser B P and Korsch R J 1988 Provenance signatures of sand–stone–mudstone suites determined using discriminant function analysis of major-element data; *Chem. Geol.* **67** 119–139.

Sharma R S 2009 *Cratons and Fold Belts of India*; Springer, Heidelberg, 304p.

Shukla A D, George B G and Ray J S 2019 Evolution of the Proterozoic Vindhyan Basin, Rajasthan, India: Insights from geochemical provenance of siliciclastic sediments; *Int. Geol. Rev.*, https://doi.org/10.1080/00206814.2019.1594412.

Singh B P, Singh Y R, Andotra D S, Patra A, Srivastava V K, Guruaribam V, Sijagurumayum U and Singh G P 2016 Tectonically driven late Paleocene (57.9–54.7 Ma) transgression and climatically forced latest middle Eocene (41.3–38.0 Ma) regression on the Indian subcontinent; *Asian Earth Sci.* **115** 124–132.

Singh N P 2007 Cenozoic lithostratigraphy of the Jaisalmer Basin, Rajasthan; *J. Paleontol. Soc. India* **52(2)** 129–154.

Singh P 2009 Major, trace and REE geochemistry of the Ganga River sediments: Influence of provenance and sedimentary processes; *Chem. Geol.* **266** 242–255.

Sun Linhua, Gui Herong and Chen Song 2012 Geochemistry of sandstones from the Neoproterozoic Shijia Formation, northern Anhui Province, China: Implications for provenance, weathering and tectonic setting; *Chemie der Erde* **72** 253–260.

Taylor S R and McLennan S M 1985 *The continental crust: Its composition and evolution*; Blackwell Scientific, Oxford, 312p.

Wu W, Zheng H, Xu S, Yang J and Liu W 2013 Trace element geochemistry of riverbed and suspended sediments in the upper Yangtze River; *J. Geochem. Expl.* **124** 67–78.

Yang Jianghai, Yuansheng D, Cawood Peter A and Xu Yajun 2012 Modal and geochemical compositions of the lower Silurian clastic rocks in north Qilian, NW China: Implications for provenance, chemical weathering, and tectonic setting; *J. Sedim. Res.* **82** 92–103.

Zachos J, Pagani M, Sloan L, Thomas E and Billups K 2001 Trends, rhythms, and aberrations in global climate 65 Ma to present; *Science* **292** 686–693.

Zachos J C, Bohaty S M, John C M, McCarren H, Kelly D C and Nielsen T 2007 The Paleocene–Eocene carbon isotope excursion: Constraints from individual shell planktonic foraminifer records; *Phil. Trans. Roy. Soc. Ser. A* **365** 1829–1842.

Corresponding editor: N V Chalapathi Rao